Journal of Materials Chemistry C

Accepted Manuscript

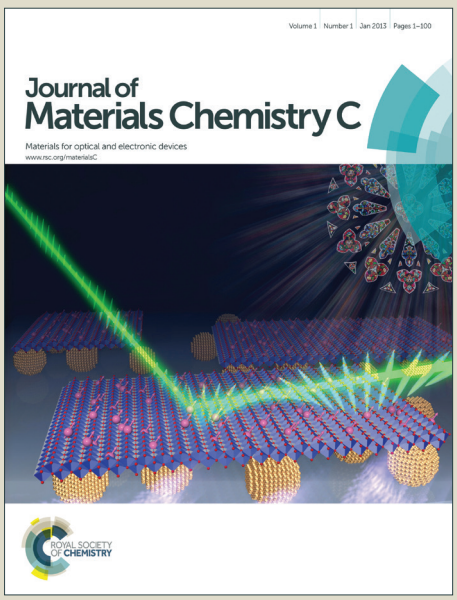

This is an *Accepted Manuscript*, which has been through the Royal Society of Chemistry peer review process and has been accepted for publication.

Accepted Manuscripts are published online shortly after acceptance, before technical editing, formatting and proof reading. Using this free service, authors can make their results available to the community, in citable form, before we publish the edited article. We will replace this *Accepted Manuscript* with the edited and formatted *Advance Article* as soon as it is available.

You can find more information about *Accepted Manuscripts* in the Information for Authors.

Please note that technical editing may introduce minor changes to the text and/or graphics, which may alter content. The journal's standard Terms & Conditions and the Ethical guidelines still apply. In no event shall the Royal Society of Chemistry be held responsible for any errors or omissions in this *Accepted Manuscript* or any consequences arising from the use of any information it contains.

ROYAL SOCIETY OF CHEMISTRY

www.rsc.org/materialsC

Journal Name

RSCPublishing

ARTICLE

Hierarchical SiO_2@Bi_2O_3 Core/Shell Electrospun Fibers for Infrared Stealthy Camouflage

Cite this: DOI: 10.1039/xoxxoooooox

Xinfang Liu,[a] Yuekun Lai,[a,c] Jianying Huang,[a] Salem S. Al-Deyab[b] and Ke-Qin Zhang[a,c]*

Received ooth January 2012,
Accepted ooth January 2012

DOI: 10.1039/xoxxoooooox

www.rsc.org/

Novel, freestanding membranes composed of SiO_2@Bi_2O_3 hierarchical core/shell fibers were prepared by a combination of two fabrication methods: electrospinning and hydrothermal reaction. The SiO_2@Bi_2O_3 composite membranes were primarily supported by flexible SiO_2 fibers after calcination treatment of electrospun PVA/SiO_2 hybrid fibrous membranes. SiO_2@Bi_2O_3 composite fibers were fabricated via a process that entails hydrothermal growth of bismuth precursor nanocoating (Bi-PN) on the surface of SiO_2 fibers followed by the thermal treatment of the harvested SiO_2@Bi-PN fibers. It was observed that Bi_2O_3 nanoparticles were well anchored on the surface of SiO_2 fibers and the phase transition of Bi_2O_3 nanoparticles occurred during the thermal treatment of SiO_2@Bi-PN composite fibers at different temperatures. The infrared emission rates of the resultant SiO_2@Bi_2O_3 composite membranes were evaluated in comparison with pure SiO_2 fibers in 2 ~ 22 μm wavebands. It is theorized that the coating of Bi_2O_3 nanoparticles contributes to the decrease of infrared emissivity, and the infrared emission properties of SiO_2@Bi_2O_3 composite fibers are related to the α-Bi_2O_3 phase. The results favourably indicated prospects of SiO_2@Bi_2O_3 composite fibrous membranes for applications in infrared stealth camouflage.

Introduction

Stealth technology is indispensable in the modern military and detection industries. Infrared stealth has become a major focus with increasing demands for advanced detection and stealth technology. Infrared detectors discover the targets by contrasting infrared radiation between the target and background. In order to implement infrared stealth camouflage, the radiation intensity difference between the target and background should be small enough that it is negligible for detection.[1] Nevertheless, the radiation intensity of most military targets is higher than that of the natural background.[2] According to the Stefan-Bolzmann's law,[3]

$$W = \varepsilon \cdot \sigma \cdot T^4 \qquad (1)$$

W: Emission energy
ε: Infrared emissivity
σ: Constant of Stefan-Boltzmann
T: Absolute temperature

the temperature(T) and infrared emissivity(ε) of the object are important parameters of infrared radiation. More specifically, infrared stealth camouflage is achieved by depressing the exterior temperature and decreasing the surface emissivity of the object.

Infrared stealth camouflage materials are a critical foundation for modern stealth technology. Infrared stealth fibers or fabrics are types of such infrared stealth materials, incorporating the infrared stealth materials into common fibers that retain the function of flexibility and weavablity. For example, a military tank warmed-up by the sun may radiate at a higher temperature than its surrounding long into a cold night and becomes easily detectable objects against the environment. Thermal-insulating materials, fiber or fibric generally acts as a cover for such objects, impeding the propagation of thermal energy. Alternatively, a low emissivity coating, polymer binder and pigment (comprised of metals, metal oxide and semiconductor) can be directly laid on the surface of the object to reduce infrared emission.[4-9] However, thick and dense coatings increase the total weight of the materials. Instead, current infrared camouflage materials are required to be thin, lightweight and possess broad band characteristics.[10-12] Via a common melt-spinning method, Yu et al.[10] prepared a bicomponent fiber with a sheath-core structure using polypropylene (PP) chips and various fillers (Ba/Mn-Zn ferrite and bronze particles). The bicomponent fiber possessed exceptional radar absorbing effect. Additionally, the bicomponent fiber possessing aluminium (Al) nanoparticles in the sheath showed better performance in radar absorption and infrared camouflage. The input of Al particles resulted in the infrared emissivity of the fibers decreasing from 0.79 to 0.62.

Over the past 20 years, electrospinning has been acknowledged as a simple but efficient method for producing fibers with diameters ranging from nano to micrometers, using a rich variety of materials (organic, inorganic or hybrid).[13-17] Moreover, electrospun mats are advantageous due to their light weight nature and large surface area. Recently, surface coating or modifications of fibers have been utilized in inorganic nanofibrous membranes for practical applications of remediation and pollution control.[18-21] The results of previous

Journal of Materials Chemistry C Accepted Manuscript

studies imply that it may be possible to fabricate composite fibers with infrared stealth performance if the fibers act as the backbone for growth of low-emissive camouflage materials. Among fibrous materials, SiO_2 nanofibrous membrane is an excellent candidate for further preparation of hierarchical structures due to its high thermal stability and good flexibility.[22] Nevertheless, SiO_2 is a conventional insulation material with high emissive. In order to achieve the lower emissivity, metallic pigments were suggested as ideal candidates[23-26] for surface coating of SiO_2 fibers. The main disadvantage is the high reflectance from the surface of metal in the visual range, which significantly reduces the visual camouflage effectiveness. Furthermore, the metal is easily oxidized at high temperatures, leading to increased emissivity.

Due to its easily controlled infrared reflection spectroscopy and emissivity, semiconductor pigment has been found broad applications in the field of infrared stealth.[27,28] Bismuth oxide (Bi_2O_3) is a semiconductor with a specific transparency and low infrared emissivity in the infrared light range. It can be used as the coating on SiO_2 fiber surfaces to reduce the emissivity of composite membranes. In addition, it is known that Bi_2O_3 exhibits polymorphism and exists in six polymorphs,[29-33] where α phase is stable at low temperature and β phase is high-temperature metastable.[34] Metastable β-Bi_2O_3 may gradually change into α-Bi_2O_3 as the treated temperature increases.[35,36] And each phase behaves in a special manner.[37-42] Therefore, it would be interesting to investigate the influence of Bi_2O_3 phase form on infrared emissivity properties of the composite fibers.

In this paper, we reported the preparation of SiO_2@Bi_2O_3 composite fibers through hydrothermal growth of bismuth precursor nanocoating (Bi-PN) on the surface of electrospun SiO_2 fibers followed by calcination at different temperatures. The incorporation of Bi_2O_3 nanoparticles with low infrared emissivity on the fibers potentially endows the fibrous membrane with properties that make it feasible for use in infrared stealth camouflage. The effects of Bi_2O_3 phase form on infrared emissivity properties of the composite fibers have been studied in the range of 2 ~ 22 μm.

Experimental

Materials. All chemicals and solvents were commercially available and used as received without further purification. The starting materials included polyvinyl alcohol (PVA, molecular weight (M_w) is from 75000 to 80000 g/mol), tetraethyl orthosilicate (TEOS), diethylene glycol (DEG, 99.0%), phosphoric acid (H_3PO_4), concentrated nitric acid, concentrated sulfuric acid, hydrogen peroxide (H_2O_2, 30%), acetone and ethanol were purchased from Sinopharm Chemical Reagent Co., Ltd., (China). Bismuth acetate (99.999%) was purchased from Alfa Aesar (Tianjin) Co., Ltd., China. Deionized (DI) water was used in all experiments.

Preparation of SiO_2 fibrous membrane. The electrospun SiO_2 fibrous membrane was produced as following procedures according to the literature.[43] 3 g of 10 wt % PVA aqueous solution was dropped slowly into an equivalent weight of silica gel which was prepared by hydrolysis and polycondensation of a mixture with the molar composition of TEOS:H_3PO_4:H_2O = 1:0.01:11. After stirring, viscous precursor solution of the PVA/SiO_2 composite was obtained. Electrospinning was conducted using a microinjection pump at constant temperature (25 °C) and relative humidity (50%). Precursor solution was transferred into a 10 mL syringe with a 21 gauge (diameter = 0.5 mm) needle. The distance between the metallic needle and a squared metallic mesh collector (a = 15 cm) was 15 cm. The hybrid fibrous membrane (PVA/SiO_2) was spun at a fixed electrical potential of 16 kV and fixed feeding rate of 1.0 mL/h precursor solution. The hybrid fibrous membrane was peeled off and then calcinated at 800 °C in air for 4 hrs to remove PVA. The fibrous membrane with the chemical composition SiO_2 was obtained. Subsequently, the as-prepared SiO_2 fibrous membrane was immersed in a bath of H_2SO_4/H_2O_2 (3:1, v/v) for about 6 hrs and thoroughly rinsed with DI water and ethanol several times.

Preparation of SiO_2@Bi-PN core/shell fibrous membrane. The synthesis process of SiO_2@Bi-PN fibers is described briefly as follows. First, 0.20 mmol (0.077 g) of bismuth(III) acetate was dissolved in diethylene glycol (DEG, 5ml) under vigorous stirring. Following this, 2 mL concentrated nitric acid and 35 mL of acetone were added. The resultant mixture solution was stirred for another 30 minutes.[44] Then, the SiO_2 fibrous membrane was immersed into the Bi-PN solution followed by hydrothermal treatment at 100 °C for 10 hrs in a Teflon-lined stainless steel vessel (50 mL). After cooling to room temperature, the obtained SiO_2@Bi-PN fibers were washed with ethanol three times and dried at 60 °C in the oven.

Preparation of SiO_2@Bi_2O_3 composite membranes. The above SiO_2@Bi-PN fibrous membranes were heated at different temperatures for 4 hrs. The resultant samples SiO_2@Bi_2O_3(400), SiO_2@Bi_2O_3(500) and SiO_2@Bi_2O_3(600) were obtained at heating temperature of 400 °C, 500 °C and 600 °C, respectively. A heating rate of 1 °C/min was used.

Characterization. Thermal property of the SiO_2@Bi-PN composite membrane was studied from 50 to 800 °C with a heating rate of 10 °C/min by a thermogravimetric analyzer (Diamond TG/DTA, PerkinElmer). The morphological analyses of the fibers were analyzed by a field emission scanning electron microscope (FE-SEM, S-4800, Hitachi) and a transmission electron microscopy (TEM, FEI Tecnai G20). All samples were coated by gold sputtering prior to SEM observations. The structural analyses of the fibers were conducted from 2θ = 10° to 60° using X-ray diffractometer (XRD, X'Pert-Pro MRD, Philips) with Cu Kα radiation (λ = 0.1542 nm) under a voltage of 40 kV and a current of 40 mA. X-ray photoelectron spectroscopy (XPS) spectra were obtained using XPS (Axis Ultra HSA, Kratos) with monochromatic Al Kα radiation at a reduced power of 225 W. For the high-resolution scan, the step size was 0.1 eV and the pass energy was 40 eV. The vacuum in the analysis chamber was maintained at 4.0×10^{-9} Pa for measurement. Infrared emission properties were examined using an infrared emission tester (TSS-5X, Japan) at room temperature. According to the Kirchhoff's law,[45] the relationship between infrared emissivity (ε) and reflectance (R) is expressed as:

$$\varepsilon + R = 1 \qquad (2)$$

The emissivity was determined by converting reflectance of infrared rays which were emitted from hemispherical black body inside a sensor head at the surface of measurement target. The standard error of the instrument is ± 0.01. The fibrous membranes were tailored into a square shape with dimensions of 50 × 50 mm^2 for measurement.

Results and discussion

Fig. 1 shows the electrospun PVA/SiO_2 hybrid fibrous membrane and SiO_2 fibrous membrane as prepared, and after bending. Notably, the SiO_2 fibrous membrane presented the high flexibility upon bending as shown in Fig. 1c and 1d. The thickness of the SiO_2 fibrous membrane, as collected, is approximately 200 μm in Fig. 2a. The morphology of SiO_2 fibers was investigated by SEM (Fig. 2b and 2c), which

Journal of Materials Chemistry C Accepted Manuscript

 This journal is © The Royal Society of Chemistry 2012

presented that the surface of SiO_2 fibers is smooth and clean, and cross-section of SiO_2 fibers are solid and compact. In addition, the average diameter of the SiO_2 fibers is approximately 800 nm. It can be seen that the crosslinkling between silica fibers, which was highlighted by the red circles

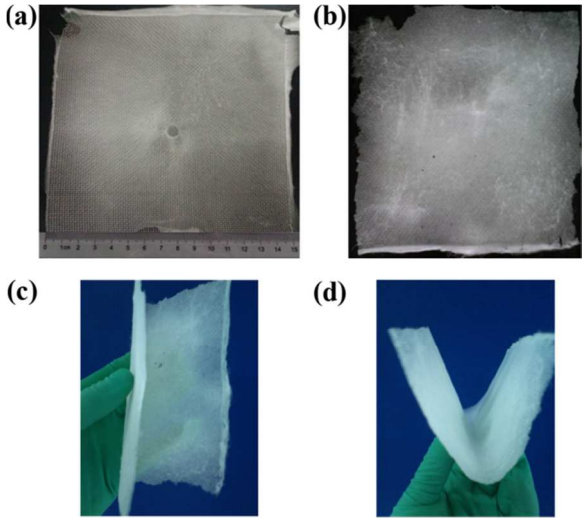

Fig. 1 Photos of (a) electrospun PVA/SiO_2 hybrid fibrous membrane on a squared metallic mesh collector (a = 15 cm) and (b) SiO_2 fibrous membrane after removing of PVA via calcination, (c) and (d) bending flexibility of the SiO_2 fibrous membrane.

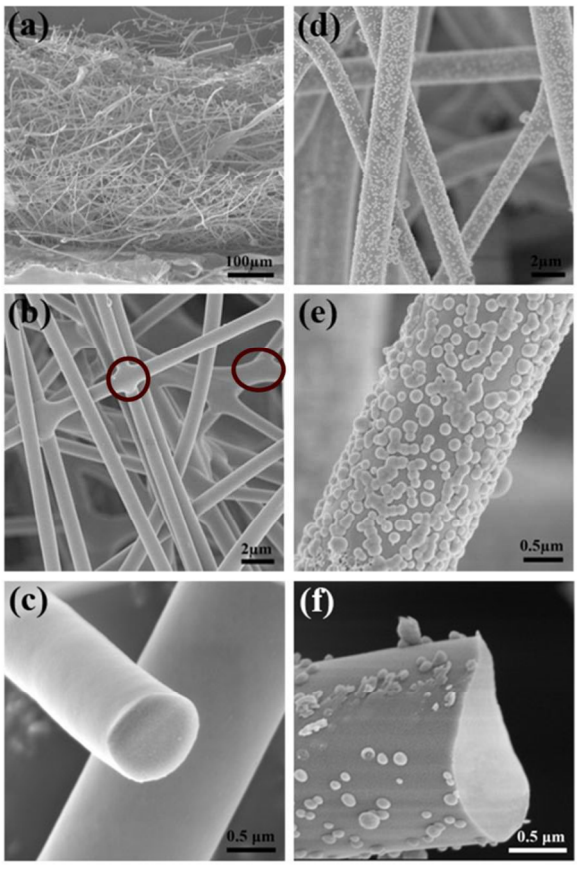

Fig. 2 SEM micrographs (a) cross-sectional view of SiO_2 fibrous membrane, (b) SiO_2 fibers, (c) cross-sectional view of SiO_2 fibers, (d) and (e) SiO_2@Bi-PN core/shell fibers at low and high magnification, (f) cross-sectional view of SiO_2@Bi-PN core/shell fibers.

in Fig. 2b. It is formed in the electrospun process and the hydroxyl groups of PVA on the surface of nanofibers interact to each other. And after calcinations, the melting phenomenon[22] may reinforce the connection. In comparison, it can be observed in Fig. 2d-2f that the nanoparticles of bismuth precursor have been fixed and uniformly dispersed only on the surface of SiO_2 fibers. The activation of SiO_2 with -OH groups increases the combination of Bi_2O_3 nanoparticles with SiO_2 fibers, liminating dependence on adhesives.

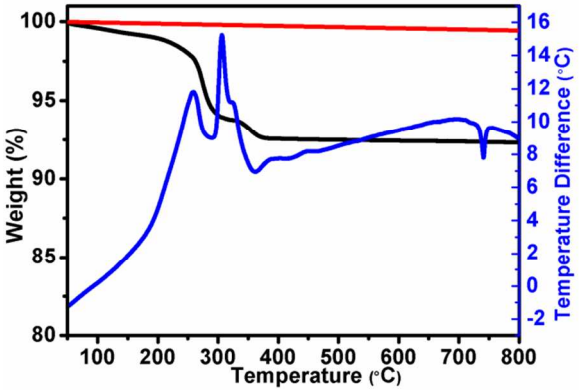

Fig. 3 The TGA of SiO_2 fibers (red) and TG-DTA of SiO_2@Bi-PN fibers (black and blue).

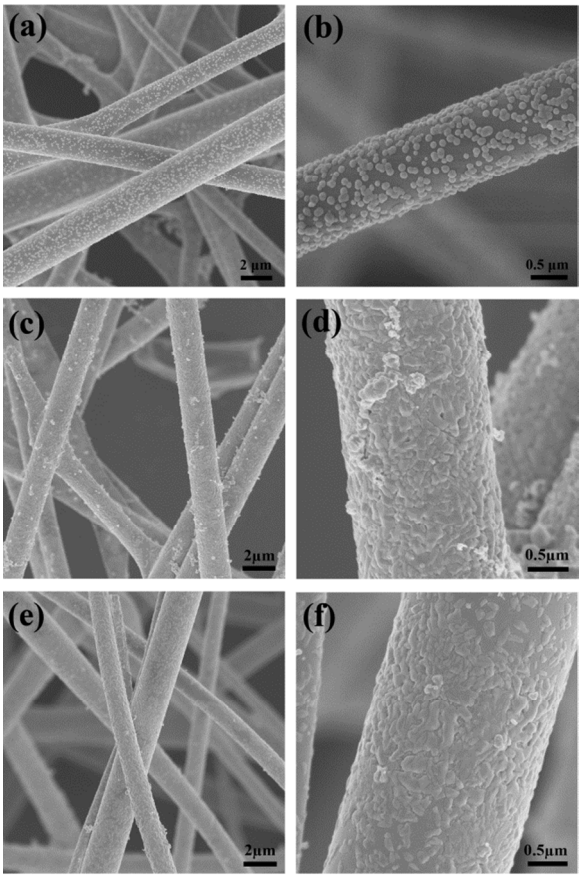

Fig. 4 SEM images of SiO_2@Bi_2O_3 composite fibers calinated at different temperatures: (a) and (b) 400 °C, denoted as SiO_2@Bi_2O_3(400), (c) and (d) 500 °C, denoted as SiO_2@Bi_2O_3(500), (e) and (f) 600 °C, denoted as SiO_2@Bi_2O_3(600).

Journal of Materials Chemistry C Accepted Manuscript

The thermal transformation of the precursor SiO_2@Bi-PN to SiO_2@Bi_2O_3 was measured based on the TGA and DTA measurements, as shown in Fig. 3. First, the SiO_2 fibers retain constant weight from 50 to 800 °C, confirming the thermal stability of the SiO_2 membrane. The TGA curve of SiO_2@Bi-PN composite membrane showed the weight loss in the range of 200-350 °C, which can be attributed to the decomposition of bismuth precursor and the phase transformation from precursor to Bi_2O_3.The temperature range of sharp peaks on DTA trace fits well with that of conversion in the TGA curve. Furthermore, the DTA curve gradually ascended as the temperature increased, which may be the evidence of Bi_2O_3 phase transition processes. According to the TGA and DTA curves, the calcination process was performed at a temperature of above 400 °C to ensure the phase transition occurred.

After being calcinated at 400°C, 500°C, and 600°C, SiO_2@Bi_2O_3 composite fibers were obtained and observed by SEM, as shown in Fig. 4. It can be seen that the Bi_2O_3 particles form separate domains with a spherical shape and diameter of 100-300 nm on the surface of SiO_2 fibers after calcination at 400 °C, which is consistent with the result of TEM observation (Fig. S1 in ESI). As the temperature increased to 500 °C, fused domains connected and covered the surface of the fibers. At 600 °C, the surfaces of the fibers were completely covered by the Bi_2O_3 layer, which possessed the higher smoothness compared with previous conditions. The difference of the morphology of SiO_2@Bi_2O_3 core-shell fibers indicates that the Bi_2O_3 may undergo phase transitions and unusual reactions as the temperature increases, resulting in different phase structures.

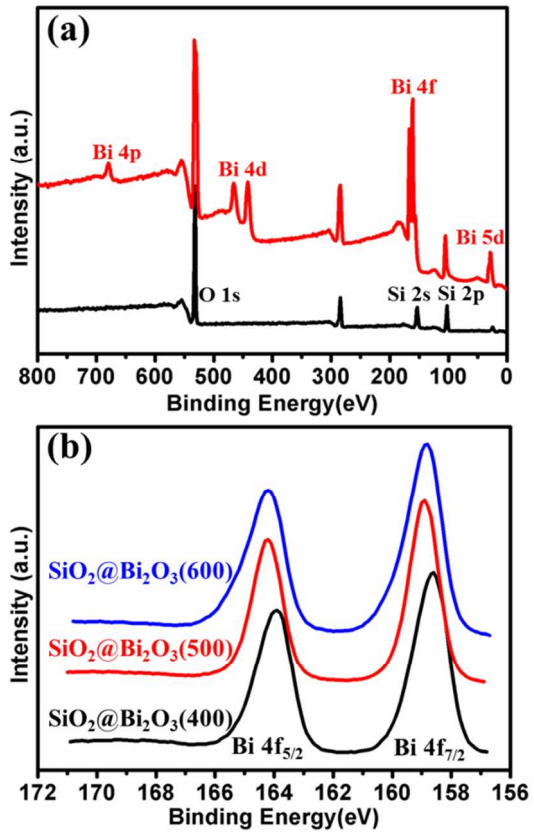

Fig. 5 (a) XPS spectra for the surface of SiO_2 fibers (black) and SiO_2@Bi_2O_3(400) composite fibers (red) for comparison. (b) High resolution spectra of Bi 4f peaks for SiO_2@Bi_2O_3 composite fibers calcinated at different temperatures.

Fig. 5a shows the XPS spectra of the representative sample SiO_2@Bi_2O_3(400) in comparison with the pure SiO_2 fibers. It can be seen that apart from the Si 2p and O 1s peaks, peaks such as Bi 4p, Bi 4d, Bi 4f, Bi 5d emerged with strong relative intensities, indicating that SiO_2 fibers were mainly coated with Bi_2O_3 particles. The C 1s peak, located at 284.5 eV in the XPS spectra, is derived from a surface layer of carbon or organic contamination. The high resolution XPS spectra of Bi 4f exhibit narrow Gauss-shaped dual peaks, denoted as Bi $4f_{7/2}$ and Bi $4f_{5/2}$ spectra, as shown in Fig. 5b. The characteristic binding energies of Bi $4f_{7/2}$ and Bi $4f_{5/2}$ are 158.6 eV and 163.9 eV for SiO_2@Bi_2O_3(400) fibers, and 158.9 eV and 164.2 eV for both SiO_2@Bi_2O_3(500) and SiO_2@Bi_2O_3(600) fibers. These values are in agreement with the reported values,[37,42] which indicate that the Bi ions are mainly in the oxidation state of Bi^{3+}. Nevertheless, the peak position of Bi 4f shifts to a higher binding energy as the calcination temperature increases from 400 to 600 °C. The shifting of binding energies confirms the change of the oxidation state of Bi ions, which may attribute to the phase transition of Bi_2O_3.

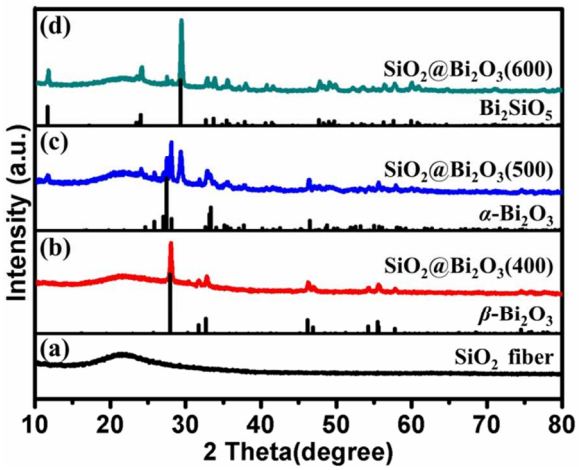

Fig. 6 XRD patterns: (a) SiO_2 fibers, (b) standard JCPDS data for β-Bi_2O_3 (black) and SiO_2@Bi_2O_3(400) composite fibers (red), (c) standard JCPDS data for α-Bi_2O_3 (black) and SiO_2@Bi_2O_3(500) composite fibers (blue), (d) standard JCPDS data for Bi_2SiO_5 (black) and SiO_2@Bi_2O_3(500) composite fibers (green).

XRD patterns of the SiO_2 fibers and composite fibers are shown in Fig. 6. The pure SiO_2 fibers show a weak and broad diffraction peak around 22°, which can be attributed to the amorphous phase of SiO_2 in Fig. 6a. In Fig. 6b, the diffraction peaks of SiO_2@Bi_2O_3 fibers are in accordance with a standard diffraction of β-Bi_2O_3 (JCPDS No. 78-1793). The sharp diffraction peaks indicate its high crystallinity. It is notable that in the XRD pattern of the SiO_2@Bi_2O_3(500) composite membrane, shown in Fig. 6c, the peaks of β-Bi_2O_3 decrease while the second phase of α-Bi_2O_3 (JCPDS No. 76-1730) and another new phase with the chemical composition Bi_2SiO_5 (JCPDS No. 75-1483) appeared. Namely, the SiO_2@Bi_2O_3(500) composite membrane is containing α-Bi_2O_3 and β-Bi_2O_3 phase junction. With the further increase of thermal treatment temperature up to 600 °C, the major phase can be indexed to the Bi_2SiO_5 while a trace amount of α-Bi_2O_3 phase as shown in Fig. 6d. It is clear that the SiO_2@Bi_2O_3 core-shell fibers undergo a phase transition from β-Bi_2O_3 to α-Bi_2O_3 and interfacial reaction of Bi_2O_3 and SiO_2[46] occur as the temperature increases from 400 to 600 °C.

Journal of Materials Chemistry C Accepted Manuscript

This journal is © The Royal Society of Chemistry 2012

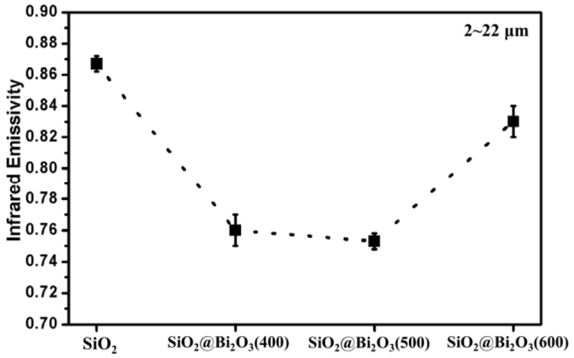

Fig. 7 Infrared emissivity of SiO_2 fibrous membrane and $SiO_2@Bi_2O_3$ composite membranes caclinated at different temperatures.

The infrared emissivity of SiO_2 fibrous membrane within the wavelength range of 2 ~ 22 μm is determined to be 0.87 (Fig. 7). For $SiO_2@Bi_2O_3$ composite membranes, there is a special layer between the core and shell interface. The motion modes of molecules, atoms and dangling bond at the interface layer are not same as those of bulk SiO_2 fibers,[47] which give rise to different infrared absorption. According to the Kirchhoff's law,[45] the emissivity is equal to the absorptivity of incident radiation for the same material. Therefore, it is observed that the infrared emission rates of $SiO_2@Bi_2O_3$ composite fibrous membranes clearly decrease compared to the pure SiO_2 fibrous membrane, which can be ascribed to the interfacial interactions between SiO_2 fibers and Bi_2O_3 particles. Particularly, the emissivity of $SiO_2@Bi_2O_3(500)$ composite membrane is estimated to be 0.75, displaying the lower infrared emissivity than that of $SiO_2@Bi_2O_3(400)$ composite membrane. It is supposed that the stable phase α-Bi_2O_3 owing to the phase transition of β-Bi_2O_3 is more beneficial for decreasing the infrared emissivity. Firstly, the β-Bi_2O_3 was formed at 400 °C, and was converted to α-Bi_2O_3 after higher calcination temperature. β-Bi_2O_3 is a metastable tetragonal phase that exists at moderate temperatures between 330 and 650 °C. It has a distorted defect structure with 25% of ordered vacant oxygen sites and could be stabilized to room temperature by partial substitution with other metal cations.[48,49] Therefore, partial replacement of Bi atoms with Si atoms may occur while the $SiO_2@Bi_2O_3(400)$ composite membrane was cooling from 400 °C to room temperature. Consequently, the lattice will be compressed around the Si impurity. Impurities are known to affect vibrational properties of crystals by modifying the distribution of normal mode frequencies and altering the nature of the atomic displacements in the neighbourhood of the impurities. The β-Bi_2O_3 with distorted lattice could enhance the infrared absorptivity. This enhancement may be also associated with CO_2 molecules in air adsorbed on these coordinatively unsaturated sites and interacted with β-Bi_2O_3 on the surface. As a result, it induces the higher infrared emissivity. In comparison, α-Bi_2O_3 displayed lower infrared emissivity owing to its stable and less-defect crystal structure. Instead of promoting complete transition from β-Bi_2O_3 to α-Bi_2O_3, the increasing of treatment temperament encourages the interfacial reaction of Bi_2O_3 and SiO_2, which gives rise to the less amount of α-Bi_2O_3 and slight higher infrared emissivity for $SiO_2@Bi_2O_3(600)$ composite fibrous membrane. In addition, the repeated measurements of infrared emissivity of $SiO_2@Bi_2O_3$ composite fibrous membranes are under the ambient condition and last for a couple of weeks. The final results show the stability within the range of fluctuation (experimental and systemic errors), which means the aging effect of the fibers is insignificant under the repeated infrared exposure.

Conclusions

In this work, we have prepared $SiO_2@Bi_2O_3$ composite fibrous membranes through a process that includes electrospinning and hydrothermal reaction, followed by calcination. Using thermal treatments at different temperatures, $SiO_2@Bi_2O_3$ composite fibrous membranes with different phase structural Bi_2O_3 were obtained. The coating of Bi_2O_3 nanoparticles contributes to the infrared emissivity of the composite fibrous membranes. And introduction of stable α-Bi_2O_3 nanoparticles to the $SiO_2@Bi_2O_3$ composite fibers could decrease the infrared emissivity of the composite membrane more effectively.

Acknowledgements

The authors thank the financial support from the National Science Foundation of China (NSFC) under Grant 51073113, 51373110 and Natural Science Foundation of the Jiangsu Higher Education Institutions of China under Grant 10KJA540046. We also acknowledge the funds from the project of the Priority Academic Program Development of Jiangsu Higher Education Institutions (PAPD), Qing Lan Project for Excellent Scientific and Technological Innovation Team of Jiangsu Province (2012) and Project for Jiangsu Scientific and Technological Innovation Team (2013). Chair professor, Salem S. Al-Deyab, extends his appreciation to the Deanship of Scientific Research at King Saud University for funding this work through the research group project (No. RGP-089). The author, Xinfang Liu, gratefully acknowledges the support of the Postdoctoral Science Foundation of Jiangsu province (No.1201030B).

Notes and references

[a] National Engineering Laboratory for Modern Silk, College of Textile and Clothing Engineering, Soochow University, Suzhou, Jiangsu 215123, China.

[b] Department of Chemistry, College of Science, King Saud University, Riyadh 11451, Saudi Arabia.

[c] Research Center of Cooperative Innovation for Functional Organic/Polymer Material Micro/Nanofabrication, Soochow University, Suzhou, Jiangsu 215123, China.

* Corresponding author's email: kqzhang@suda.edu.cn.

Electronic Supplementary Information (ESI) available: TEM images of $SiO_2@Bi_2O_3$ composite fibers. See DOI: 10.1039/xoxxoooooox/

1 T. Hallberg, T. Niinimaeki-Heikkilae, E. Hedborg-Karlsson, P. S. Salonen, C. Nilsson and A. Jaenis, *Development of Low-Emissive Camouflage Paint: Final Report*, Scientific Report, FOI-R-1592-SE, 2005.

2 L. G. Karlsson, *US Pat.*, 4 529 633, 1985.

3 D. P. Sheehan, *Entropy*, 2012, **14**, 1915-1938.

4 C. C. Yang, Y. J. Gung, W. C. Hung, T. H. Ting and K. H. Wu, *Composites Science and Technology*, 2010, **70**, 466-471.

5 R. F. Supcoe, *US Pat.*, 4 311 623, 1982.

6 C. R. Sutter, *US Pat.*, 6 468 647, 2002.

7 P. K. Biswas, A. De, N. C. Pramanik, P. K. Chakraborty, K. Ortner, V. Hock and S. Korder, *Mater. Lett.*, 2003, **57**, 2326-2332.

Journal of Materials Chemistry C Accepted Manuscript

8 W. Zhang, G. Xu, R. Ding, K. Duan and J. Qiao, *Mater. Sci. Eng. C.*, 2013, **33**, 99-102.
9 H. Yu, G. Xu, X. Shen, X. Yan and C. Cheng, *Appl. Surf. Sci.*, 2009, **255**, 6077-6081.
10 B. Yu, L. Qi, J.-Z. Ye and H. Sun, *J. Appl. Polym. Sci.*, 2007, **104**, 2180-2186.
11 J. Zhou, J. He, G. Li, T. Wang, D. Sun, X. Ding, J. Zhao and S. Wu, *J. Phys. Chem. C*, 2010, **114**, 7611-7617.
12 L. Chen, C. Lu, Y. Lu, Z. Fang, Y. Ni and Z. Xu, *RSC Adv.*, 2013, **3**, 3967-3972.
13 D. Li and Y. N. Xia, *Adv. Mater.*, 2004, **16**, 1151-1170.
14 A. Greiner and J. H. Wendorff, *Angew. Chem., Int. Ed.*, 2007, **46**, 5670-5730.
15 W. E. Teo and S. Ramakrishna, *Nanotechnology*, 2006, **17**, R89-R106.
16 Z. M. Huang, Y. Z. Zhang, M. Kotaki and S. Ramakrishna, *Compos. Sci. Technol.*, 2003, **63**, 2223-2253.
17 D. H. Reneker and A. L. Yarin, *Polymer*, 2008, **49**, 2387-2425.
18 R. Wang, J. Guo, Y.-E. Miao, J. Pan, W. W. Tjiu and T. J. Liu, *J. Mater. Chem.*, 2011, **21**, 19375-19380.
19 Y.-E. Miao, R. Wang, D. Chen, Z. Liu and T. Liu, *ACS Appl. Mater. Interfaces*, 2012, **4**, 5353-5359.
20 X. Mao, Y. Chen, Y. Si, L. yang, H. Wan, J. Yu, G. Sun and B. Ding, *RSC Adv.*, 2013, **3**, 7532-7569.
21 Y. Chen, X. Mao, H. Shan, J. yang, H. Wang, S. Chen, F. Tian, J. Yu and B. Ding, *RSC Adv.*, 2014, **4**, 2756-2763.
22 X. Mao, Y. Si, Y. Chen, L. yang, F. Zhao, B. Ding and J. Yu, *RSC Adv.*, 2012, **2**, 12216-12223.
23 C. Cagran and G. Pottlacher, *J. Non-Cryst. Solids*, 2007, **353**, 3582-3586.
24 W. Zhang, G. Xu, R. Ding, K. Duan and J. Qiao, *J. Mater. Sci. Eng. C.*, 2013, **33**, 99-102.
25 H. Yu, G. Xu, X. Shen, X. Yan and C. Cheng, *Appl. Surf. Sci.*, 2009, **255**, 6077-6081.
26 G. Wu and D. Yu, *Infra. Phys. Tech.*, 2012, **55**, 26-31.
27 S.-Y. Zhang, Q.-X. Cao and Y.-H. Yao, *Infrared Physics & Technology*, 2013, **61**, 1-4.
28 X. Su, Y. Jia, X. Liu, J. Wang, J. Xu, X. he, C. Fu and S. Liu, *Ceram. Inter.*, 2014, **40**, 5307-5311.
29 H. Deng, W. C. Hao and H. Z. Xu, *Chin. Phys. Lett.*, 2011, **28**, 056101.
30 Y. Qiu, M. Yang, H. Fan, Y. Zuo, Y. Shao, Y. Xu, X. Yang and S. Yang, *Mater. Lett.*, 2011, **65**, 780-782.
31 C. L. Gomez, O. Depablos-Rivera, J. C. Medina, P. Silva-Bermudez, S. Muhl, A. Zeinert and S. E. Rodil, *Solid State Ionics*, 2014, **255**, 147-152.
32 L.-C. Tien and Y.-C. Lai, *Appl. Surf. Sci.*, 2014, **290**, 131-136.
33 Q. Huang, S. Zhang, C. Cai and B. Zhou, *Mater. Lett.*, 2011, **65**, 988-990.
34 M. Drache, P. Roussel and J. P. Wignacourt, *Chem. Rev.*, 2007, **107**, 80-96.
35 O. Monnereau, L. Tortet, P. Llewellyn, F. Rouquerol and G. Vacquier, *Solid State Ionics*, 2003, **157**, 163-169.
36 C. Wang, C. Shao, L. Wang, L. Zhang, X. Li and Y. J. Liu, *Colloid Interface Sci.*, 2009, **333**, 242-248.
37 H. F. Cheng, B. B. Huang, J. B. Lu, Z. Y. Wang, B. Xu, X. Y. Qin, X. Y. Zhang and Y. Dai, P*hys. Chem. Chem. Phys.*, 2010, **12**, 15468-15475.
38 H. Deng, W. Hao, H. Xu and C. Wang, *J. Phys. Chem.*, 2012, **116**, 1251-1255.
39 Y. Qiu, D. Liu, J. Yang and S. Yang, *Adv. Mater.*, 2006, **18**, 2604-2608.
40 Y. Sun, W. Wang, L. Zhang and Z. Zhang, *Chem. Eng. J.*, 2012, **211-212**, 161-167.
41 J. Hou, C. Yang, Z. Wang, W. Zhou, S. Jiao and H. Zhu, *Appl. Catal. B: Environ.*, 2013, **142-143**, 504-511.
42 R. Li, W. Chen, H. Kobayashi and C. Ma, *Green Chem.*, 2010, **12**, 212-215.
43 M. Guo, B. Ding, X. Li, X. Wang, J. Yu and M. Wang, *J. Phys. Chem. C*, 2010, **114**, 916-921.
44 C. C. Li and H. C. Zeng, J. Am. Chem. Soc. 2012, 134, 19084-19091.
45 S. Enoch, J. J. Simon, L. Escoubas, Z. Elalmy, F. Lemarquis, P. Torchio and G. Albrand, *Appl. Phys. Lett.*, 2005, **86**, 261101.
46 H. W. Guo, X. F. Wang and D. N. Gao, *Mater. Lett.*, 2012, **67**, 280-282.
47 R. J. Davis and Z. Liu, *Chem. Mater.*, 1997, **9**, 2311-2324.
48 D. Barreca, F. Morazzoni, G. A. Rizzi, R. Scotti and E. Tondello, *Phys. Chem. Chem. Phys.*, 2001, **3**, 1743-1749.
49 Y. Wang, Y. Wen, H. Ding and Y. Shan, *J. Mater. Sci.*, 2010, **45**, 1385-1392.

Journal of Materials Chemistry C Accepted Manuscript

This journal is © The Royal Society of Chemistry 2012

TOC

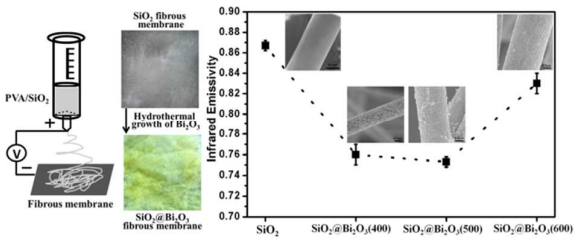

Hierarchical SiO_2@Bi_2O_3 core/shell electrospun fibrous membranes with low infrared emissivity were successfully prepared. And the infrared emissivity is influenced by the Bi_2O_3 nanoparticles with different phase structures on the surfaces of the SiO_2 fibers.

Journal of Materials Chemistry C Accepted Manuscript